NeuroImage: Clinical 19 (2018) 396–405

Contents lists available at ScienceDirect

NeuroImage: Clinical

journal homepage: www.elsevier.com/locate/ynicl

Subthalamic oscillatory activity and connectivity during gait in Parkinson's disease

Franz Hell[a,c,*], Annika Plate[a,c], Jan H. Mehrkens[b], Kai Bötzel[a,c]

[a] Department of Neurology, Ludwig-Maximilians-Universität München, Marchioninistr. 15, D-81377 Munich, Germany
[b] Department of Neurosurgery, Ludwig-Maximilians-Universität München, Marchioninistr. 15, D-81377 Munich, Germany
[c] Graduate School of Systemic Neurosciences, GSN, Ludwig-Maximilians-Universität München, Grosshadernerstr. 2, D-82152 Martinsried, Germany

ARTICLE INFO

Keywords:
Deep brain stimulation
Subthalamic nucleus
Gait
Oscillations
Beta rhythm

ABSTRACT

Local field potentials (LFP) of the subthalamic nucleus (STN) recorded during walking may provide clues for determining the function of the STN during gait and also, may be used as biomarker to steer adaptive brain stimulation devices. Here, we present LFP recordings from an implanted sensing neurostimulator (Medtronic Activa PC + S) during walking and rest with and without stimulation in 10 patients with Parkinson's disease and electrodes placed bilaterally in the STN. We also present recordings from two of these patients recorded with externalized leads. We analyzed changes in overall frequency power, bilateral connectivity, high beta frequency oscillatory characteristics and gait-cycle related oscillatory activity. We report that deep brain stimulation improves gait parameters. High beta frequency power (20-30 Hz) and bilateral oscillatory connectivity are reduced during gait, while the attenuation of high beta power is absent during stimulation. Oscillatory characteristics are affected in a similar way. We describe a reduction in overall high beta burst amplitude and burst lifetimes during gait as compared to rest off stimulation. Investigating gait cycle related oscillatory dynamics, we found that alpha, beta and gamma frequency power is modulated in time during gait, locked to the gait cycle. We argue that these changes are related to movement induced artifacts and that these issues have important implications for similar research.

1. Introduction

Recordings of local field potentials (LFP) in the basal ganglia of patients with Parkinson's disease (PD) have demonstrated oscillations at several frequencies, of which the beta band has gained most attention (Stein and Bar-Gad, 2013). Although the functional and pathological role of (beta) oscillations are still debated (Espenhahn et al., 2017; Eusebio and Brown, 2009; Gross et al., 2005; Pfurtscheller et al., 1996; Raz et al., 1996), beta power has been shown to be correlated with akinetic-rigid symptoms (Hammond et al., 2007; Kühn et al., 2006b; Neumann et al., 2016) in human patients as well as in animal models of parkinsonism (Costa et al., 2006; Mallet et al., 2008; Sharott et al., 2005). Beta oscillations are also reported to be reduced in amplitude after levodopa intake and are attenuated by STN deep brain stimulation (DBS) in a stimulation intensity dependent manner (Kühn et al., 2008a, 2008b; Oswal et al., 2016; Quinn et al., 2015; Trager et al., 2016; Weiss et al., 2015).

Local field potentials are investigated as biomarkers for adaptive closed-loop stimulation in PD (Cagnan et al., 2013; Johnson et al., 2016; Little et al., 2013a; Piña-Fuentes et al., 2017; Tinkhauser et al., 2017a). When considering oscillatory activity as a feedback signal, it is important to understand its functional role as well as its contributions to the genesis of clinical symptoms. Cortical as well as subcortical beta has been shown to be involved in a series of neural processes underlying cognitive functioning and motor behavior (Frank, 2006; Frank et al., 2007; Herz et al., 2017a; Meijer et al., 2016; Tan et al., 2014a, 2014b; Te Woerd et al., 2015; Williams et al., 2005; Zavala et al., 2013). Beta modulations are reported to be correlated with decision thresholds and reaction times as well as with grip force (Hell et al., 2018; Herz et al., 2017b; Tan et al., 2016). Beta is decreased in amplitude during motor imagery (Kühn et al., 2006a; Marceglia et al., 2009) and movements (Joundi et al., 2013; Kühn et al., 2004; Litvak et al., 2012), while this mechanism probably fails as bradykinesia increases (Steiner et al., 2017). While beta power is attenuated prior, during and shortly after movements followed by a rebound after movement termination, low frequencies in the theta range and gamma frequencies exhibit increases at movement onset (Cassidy et al., 2002; Chung et al., 2001; Foffani et al., 2005, 2003; Fogelson et al., 2005; Kane et al., 2009; Özkurt et al., 2011; Priori et al., 2002; Tan et al., 2014a, 2014b).

Reports of beta band suppression during movement are ubiquitous,

* Corresponding author at: Department of Neurology, Ludwig-Maximilians-University, Marchioninistrasse 15, D-81377 Munich, Germany.
E-mail address: Franz.Hell@med.uni-muenchen.de (F. Hell).

https://doi.org/10.1016/j.nicl.2018.05.001
Received 28 February 2018; Received in revised form 24 April 2018; Accepted 1 May 2018
Available online 03 May 2018

but investigations of the modulation of beta during gait are rare and conflicting (Quinn et al., 2015; Singh et al., 2013; Storzer et al., 2017). Quinn et al. report that subthalamic beta power was relatively similar during lying, sitting, standing, and during forward walking and that akinetic-rigid PD subjects tended to exhibit decreased beta power when walking, while tremor dominant subjects did not. Storzer et al. report, that patients without freezing of gait show a suppression of beta power in both bicycling and walking, while this suppression was stronger for bicycling. Both Singh and Storzer report a movement-induced, narrowband power increase in the low beta band during walking in patients with freezing of gait, time-locked to the onset of gait.

In this study, we used a sensing neurostimulator (Activa PC + S®, Medtronic, plc.) connected to electrodes implanted bilaterally in the STN's of 10 patients with PD as well as recordings from externalized leads in two of the same patients. We investigated subthalamic oscillatory activity during continuous gait, while also comparing neural activity during gait and sitting and standing rest. Recordings were made off stimulation, with stimulation at half the clinical most beneficiary amplitude and stimulation with full amplitude. Kinematic parameters were recorded with inertial sensor units and subsequently analyzed in parallel to the electrophysiological activity to reconstruct gait-cycle related oscillatory activity. Our main aim was to discuss whether and how subthalamic frequency content changes during walking across the gait cycle as compared to rest.

2. Material and methods

2.1. Patients, surgery, electrode localization

Ten participants with a mean age of 61.7 years (SEM ± 2.1), including 9 males and one female patient with Parkinson's disease (PD) took part in this study and gave their written informed consent. The protocol was approved by the Ethics Committee of the medical faculty of the University of Munich. Clinical details of all participants are provided in Table 1. All patients underwent implantation of DBS leads (model 3389; Medtronic Neurological Division, MN, USA) with 4 ring electrodes in the left and right STN for the treatment of advanced Parkinsonism at the Department of Neurosurgery at the hospital of the University of Munich. Initial stereotactic coordinates were 12 mm lateral, 3 mm posterior and 4 mm below the midpoint of the AC-PC line. Coordinates were adjusted by direct visualization of the STN on individual pre-operative T2-weighted MRI scans. Intraoperative single cell recordings and macrostimulation guided the final placement of the electrode leads. The exact position of the DBS electrodes in relation to the subthalamic target structures were determined based on the pre-operative T2-weighted MRI and postoperative CT scans, using the Lead DBS toolbox (Horn and Kühn, 2015) and 3DSlicer software (www.slicer.org). MRT and CT were aligned manually using 3DSlicer software, co-registered using a two-stage linear registration (rigid followed by affine) as implemented in Advanced Normalization Tools (Avants et al., 2008) and normalized to MNI space (MNI ICBM Nonlinear 2009b template), (Fonov et al., 2011). To visualize the STN, we used an atlas to outline the STN and its putative subdivisions, the motor, the associative and the limbic area (Accolla et al., 2014).

2.2. LFP recordings and kinematic measurements

In all patients, the leads were connected to the implanted sensing neurostimulator (Activa PC + S®, Medtronic, plc.) to record LFP's bipolarly from the electrode contact above and below the single negative stimulation contact, colored in light red (Fig. 1). The stimulation contact was chosen according to best clinical outcome. All LFP data were sampled at 422 Hz. We additionally recorded LFP data from externalized leads during the same conditions in two of these patients before implantation of the neurostimulator. Here, sutbhalamic LFP were recorded from the four contacts of the implanted stimulation electrodes in bipolar fashion using Brain Vision Recorder software and Brainamp amplifiers (Brain Products GmbH, Gilching, Germany). The bipolar pair containing the later stimulation electrode was chosen for evaluation. The experiments with externalized recording were performed two days after the initial surgery and the experiments with internal sensing equipment were performed at least 2 months after initial programming on the same or on consecutive days within the first year after implantation. We had to exclude recordings from one subject, as the LFP's were severely contaminated with ECG artifacts.

Movement parameters were recorded using inertial sensor units. We used a research prototype measurement and recording system with one analog gyroscope (IDG500, Invensense, Sunnyvale, CA, USA) and two analog accelerometers (ADXL335, Analog devices, Norwood, MA, USA) on each shank and each thigh to record kinematic profiles. Data were collected by a microprocessor (ATXMEGA 128, Atmel, San Jose, CA, USA) with 16 analog-digital converters (12-bit) connected to an SD-card for data storage. Data from the sensors were collected at 200 Hz. Synchronization of gait and LFP data was achieved by a transcutaneous electric nerve stimulator (TENS) device which was triggered at the beginning and before the end of the recording by the gait recording processor and delivered electric impulses between right mastoid and left shoulder which were recorded by the neurostimulator.

2.3. Task design

LFPs were recorded during sitting (2 min), standing rest (2 min) and free walking (approx. 125 m) along a hallway. Experiments were recorded following overnight withdrawal of dopaminergic medication

Table 1
Clinical details.
Ten patients with Parkinson's disease (1 female, mean age 61.7 ± 2.1 years; disease duration 9.8 ± 0.9 years) were studied 1 month – 1 year after DBS surgery.

Case	Age	Gender	Disease duration	Main symptoms	UPDRS-III ON/OFF	Tremor ON/OFF	Rigor ON/OFF	Gait ON/OFF	Lateralization Right/left
1	66	m	9	Equivalent	51/78	0/5	5/10	2/3	25/20
2	64	m	16	AR	23/73	0/0	3/9	1/3	23/20
3	61	m	8	TD	17/44	11/24	1/5	1/2	16/10
4	54	f	8	Equivalent	10/27	3/6	1/5	1/1	13/6
5	71	m	12	Equivalent	22/38	9/10	4/5	1/1	11/14
6	53	m	12	Equivalent	4/27	0/6	0/5	1/1	13/6
7	70	m	8	AR	23/40	0/0	7/11	1/2	15/15
8	55	m	7	Equivalent	15/33	4/10	3/8	1/2	3/12
9	66	m	11	Equivalent	26/75	6/18	1/12	2/2	7/11
10	57	m	7	AR	30/53	0/0	5/13	1/1	10/9

Evaluation was performed OFF medication after overnight withdrawal from dopaminergic medication in random order (ON/OFF DBS); Tremor score reflects the total score on all ratings in items 15–18 in the UPDRS III, rigor score reflects all ratings on item 3 and gait item 10, lateralization score reflects all scores that allow for the assessment of lateralization of Parkinsonian symptoms, including item 3–8, 15–17.

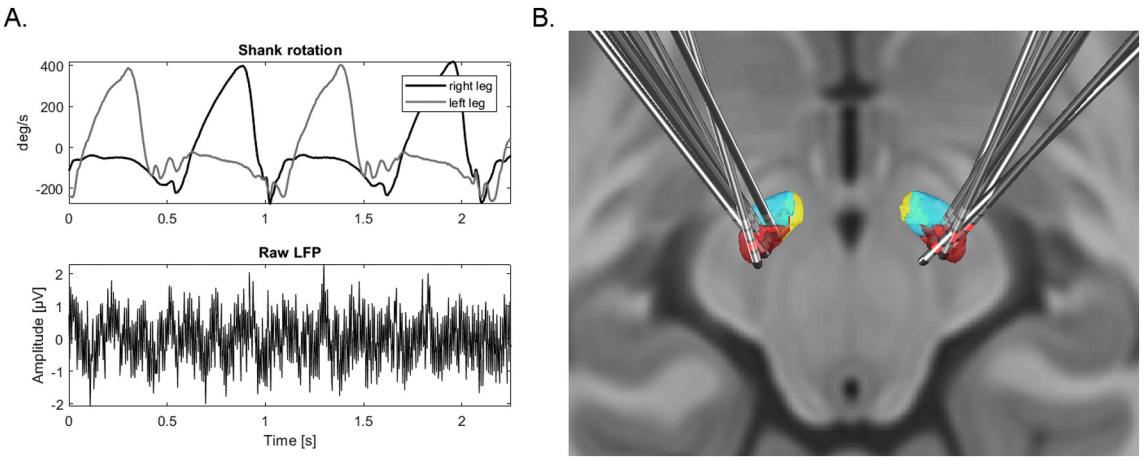

Fig. 1. Shank rotation measurements, raw LFP recordings and electrode localization. A. Shank rotation velocity of two different goniometer sensors setups mounted at right and left leg of one patient during walking and raw LFP trace from a single STN recording with Activa PC + S sensing. B. Posterior dorsal view of DBS-electrode localizations in left and right STN. The motor region of the STN is depicted in dark red, the associative subregion in light blue and limbic subregion in yellow. The contact used for stimulation is colored in light red (see text for details). (For interpretation of the references to color in this figure, the reader is referred to the web version of this article.)

and with and without DBS. DBS state (on/half/off) was changed approximately 30 min before each recording session. We conducted experiments without stimulation and with two different stimulation intensities: stimulation at the clinical optimal amplitude and half that amplitude. Stimulation frequency was 140 Hz and pulse duration was 60 µs for all recordings. Participants were asked to walk along a corridor with slow and normal speed, turn at the end and walk back. The turn was excluded from further analysis.

3. Analysis

3.1. Analysis of kinematic measurements

First, kinematic signals were re-sampled off-line to 422 Hz to match the LFP sampling frequency. Then, rotational positions of shank and thigh were computed by Kalman filtering and the trajectory of the feet were reconstructed using a 4-segment leg model with inverse kinematics. Terminal contact (TC), peak and initial contact (IC) were defined in the shank rotational velocity signal as described previously (Bötzel et al., 2016). We used the shank rotational velocity signal to visualize the gait cycle and calculated the parameters stride length, gait velocity and foot clearing to describe the gait cycle (Bötzel et al., 2018). For statistical evaluation we computed a Wilcoxon signed rank test to test for differences between conditions. We corrected the resulting p-values with False Discovery Rate (FDR) correction for multiple comparisons (Benjamini and Yekutieli, 2005; Groppe et al., 2011). Kinematic parameters with and without stimulation during slow and normal gait are reported in Supplementary materials.

3.2. Analysis of spectral power during gait and rest

We only included recordings from Activa PC + S in the analysis, except time frequency single subject analysis. All continuous recordings were divided into equal epochs with durations of 2 s. The epochs were visually inspected for artifacts; epochs containing artifacts were discarded if they exceeded an amplitude threshold set manually for each STN recording, determined from the rest recordings. We then calculated the frequency power spectrum using fast Fourier-transform-based methods (Matlab function fft) and subsequently averaged over across all epochs for each nucleus. In order to control for between nucleus differences in frequency power, which can be influenced by proximity of the electrode to the LFP source and the local electrical properties of the surrounding tissue (Neumann et al., 2016), we calculated the relative power spectrum for each recording separately. To calculate the relative spectrum, we normalized each recording by its own overall mean power across frequencies, excluding low frequencies (up to 10 Hz) and other frequencies with possible technical artifact contamination related to the sensing equipment (33–37 Hz, 48–52 Hz, 90 + Hz) (Neumann et al., 2016; Singh et al., 2013; Storzer et al., 2017). To assess the effect of gait on the frequency spectrum, we conducted a one-way ANOVA with the factors gait and rest to test for differences between the average relative power in the high beta frequency band (20–30 Hz) in each nucleus, followed by a Wilcoxon signed rank test. We applied the same procedure to the factors slow gait and standing rest. To confirm this analysis, we also investigated the change of average absolute high beta power (20–30 Hz) during normal gait in % relative to sitting rest baseline across subjects, averaged across bilateral nuclei. For statistical evaluation we computed a one-sample *t*-test.

3.3. Instantaneous amplitude extraction

The following analyses use the instantaneous amplitude (amplitude envelope) of frequency specific activity. We used a butterworth band-pass filters (Matlab function butter, filter order 5, zero-phase filtering) and the Hilbert transform to extract the instantaneous amplitude (amplitude envelope) and power across time at frequencies from 3 until 100 Hz with steps of 1 Hz.

3.4. Bilateral STN amplitude-amplitude correlations

For amplitude-amplitude correlations, we computed Pearson's correlation coefficients (R) (Arnulfo et al., 2015) between bilateral STN amplitude envelope time series across frequencies, while excluding time periods with possible artifact contamination. The correlation coefficient ranges from −1 to 1, with 0 indexing absence of correlation to 1 for perfect linear relationship and −1 for perfect anticorrelation. Correlation measures were computed separately for each subject and each resting and walking condition. To assess the modulatory effect of gait on the high beta amplitude-amplitude correlations across subjects, we conducted a one-way ANOVA to test for differences between the average correlations in the high beta frequency band (20–30 Hz) during normal gait and sitting rest without stimulation, followed by a Wilcoxon signed rank test. We applied the same procedure for testing slow gait against standing rest.

3.5. Life- and waiting-times analysis of high beta oscillation bursts

To analyze characteristics of oscillatory bursts, for each frequency and nucleus, we determined bursts based on a common median amplitude threshold across sitting rest and gait recordings, similar to recent research (Tinkhauser et al., 2017b). The epoch in which the amplitude envelope is above this threshold is considered the lifetime of a burst and the epochs below are termed waiting-times. The procedure to extract life- and waiting-times has been previously described by Montez et al. (2009). A life-/waiting-time ratio (LWR) over 1 indicates that oscillatory bursts above the threshold are longer in duration than the time-periods in which the amplitude does not cross the threshold. To evaluate the modulatory effect of gait on the high beta LWR across nuclei, we conducted a one-way ANOVA to test for differences between the average LWR in the high beta frequency band (20-30 Hz) during normal gait and sitting rest, followed by a Wilcoxon signed rank test.

3.6. High beta burst-shape analysis

To further investigate the nature of oscillatory bursts during gait as compared to rest, we studied the average shape of high beta bursts (Feingold et al., 2015). To find bursts, we marked each peak of the average high beta amplitude envelope (Matlab function findpeaks) and averaged across all bursts from each nucleus and condition using the timeframe of ± 30 ms around the peak. For statistical testing we used the average amplitudes across the whole epoch from each nucleus and condition for comparison. To test for differences between normal gait and sitting rest, we used a Friedman test followed by a Wilcoxon signed rank test, as data was not normally distributed (Kolmogorow-Smirnow-Test).

3.7. Gait-cycle related time-frequency power analysis

To reconstruct gait-cycle related oscillatory activity, we time-warped the shank rotational signal and the squared amplitude time course at each frequency from each gait cycle epoch, pragmatically defined as the epoch between two succeeding peaks of the rotational signal of one leg (Fig. 3A, Supplementary Fig. 3E, F). All epochs were re-sampled to a common timeframe of 100 samples, and averaged across epochs. To construct a sitting baseline, we used the same method, replacing the recordings made during gait with those during rest. For each nucleus we then calculated the mean percentage change between the gait time-frequency decomposition and the average baseline during sitting rest and gait across time for all frequencies and time points. For group analysis we then averaged across nuclei and then across subjects. For epochs starting and ending with the left leg mid-swing peak (e.g. Supplementary Fig. 3E), we used the time-frequency decomposition of the LFP from the right STN (e.g. Supplementary Fig. 3A) and vice versa (“contralateral averaging”).

To assess group differences in oscillatory activity between gait and rest across the gait cycle statistically, we first calculated the z-statistics for each time-frequency point separately (using Matlab function signrank) using individual time-frequency power averages across left and right nuclei. We considered the true z-value significant if it surpassed the 95% percentile of the z-statistic distribution established by testing 10,000 surrogate datasets, generated by shuffling between gait and rest averages across participants, for differences. We only considered clusters with > 20 adjacent time-frequency samples significant (Maris et al., 2007; Maris and Oostenveld, 2007).

To investigate lateralization of oscillatory activity during gait, we repeated the epoching and averaging procedure, this time using the LFP from the ipsilateral STN for the respective epochs (“ipsilateral averaging”). To compare and evaluate results, we also analyzed single subject data from recordings with externalized leads in the same fashion. We did not add these data to the group analysis.

4. Results

4.1. Patient details and localization of DBS leads

We could confirm stimulation and recording sites for all but two patients (Fig. 1). We had to exclude two subjects from localization; one subject only had a post-operative MRI image which did not allow proper electrode localization, while proper registration of MRI and post-operative CT wasn't possible in another subject because of a deformed CT scan. All but two of the analyzed stimulation contacts were placed within the motor STN (with distances between each contact center and nearest atlas voxel center below 0.5 mm). The other two had a distance of 0.9 mm and 0.54 mm and were located behind the posterior part of the STN. Overall, a mean distance of 0.19 mm (SEM ± 0.02) between each stimulation contact center and nearest atlas voxel center in the motor STN was found.

Confirming the electrode localizations, stimulation amplitudes were within normal ranges. In the condition full amplitude stimulation, which resembles clinical optimal voltage intensity, a mean constant voltage of 2.71 (± 0.15 mV) was observed on the group level. Furthermore, our cohort benefitted from stimulation as evidenced by significantly lower UPDRS-III scores with stimulation as compared to without stimulation (Wilcoxon signed rank test, $p = 0.002$, see Table 1 for clinical details) and a betterment in gait parameters (see Supplementary Fig. 1, results and discussion) with stimulation. Although patients showed minor gait impairments with varying degrees (see Table 1 for UPDRS-III scores), all patients were able to walk regularly without problems for extended periods of time.

4.2. High beta band oscillatory activity is attenuated during gait

The power-spectrum shows a significant effect in the high beta frequency range (20-30 Hz) (Fig. 2A). The average relative power in this band is reduced in amplitude during all walking conditions as compared to all resting conditions. An ANOVA with the factor task (sitting rest/normal gait) showed a significant main effect of task ($F(1, 36) = 12.38$, $p = 0.001$) on high beta band power across nuclei. A follow up Wilcoxon signed rank test confirmed significant differences ($p < 0.0001$). This difference was also significant between standing rest and slow gait ($F(1, 36) = 4.91$, $p = 0.03$; Wilcoxon signed rank test: $p < 0.0001$). No significant change was found in other frequency ranges. To supplement the relative power analysis approach and confirm results across subjects, we calculated the percent change in oscillatory power from normal gait to sitting rest in the high beta frequency range for each participant, averaging over left and right STN beforehand. Group mean percentage change from normal gait to sitting rest showed a significant attenuation of spectral power during gait as compared to rest in the high beta frequency range without stimulation (one sample *t*-test; $t(9) = -6.5$, $p = 0.0001$; mean = −39.2% ± 6%).

4.3. High beta band bilateral amplitude correlations are reduced during gait

To evaluate gait-related changes in oscillatory connectivity, we compared bilateral subthalamic amplitude envelope correlations across frequencies between rest and gait (Fig. 2B). The amplitude-correlation spectrum shows a distinct effect in the high beta frequency range (20–30 Hz). Correlations are reduced in strength during walking as compared to rest. An ANOVA with the factor task (sitting rest/normal gait) showed a significant main effect of task ($F(1, 18) = 6.72$, $p = 0.02$) on average amplitude-amplitude correlations in the high beta band (20-30 Hz) across all remaining 9 participants with bilateral recordings without ECG. A follow-up Wilcoxon signed rank test confirmed significant differences ($p < 0.01$). We also evaluated differences in amplitude correlations during slow gait and standing rest. An ANOVA with the factor task (standing rest/slow gait) confirmed results with a significant main effect of task ($F(1, 18) = 6.72$, $p = 0.02$ Wilcoxon

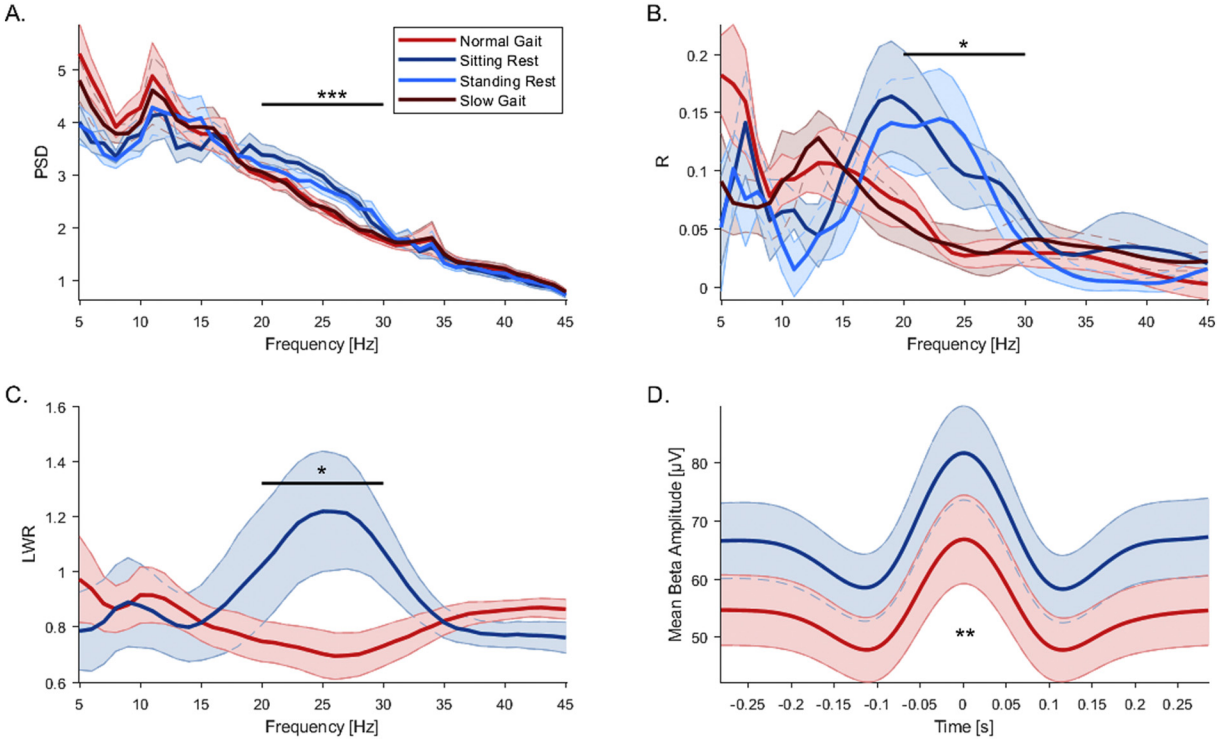

Fig. 2. Oscillatory bilateral STN frequency power, connectivity and burst analysis. A. Group relative power spectrum showing a significant difference in the high beta band 20–30 Hz. High beta power during sitting and standing rest is comparable and is attenuated during normal and slow gait. B. Group amplitude envelope correlations across frequencies between left and right STN showing significant differences between rest and gait in the high beta band. C. LWR of oscillatory bursts across frequencies during gait and sitting rest showing significant differences in the high beta band. Lifetimes of beta bursts are prolonged during rest and waiting-times are shortened as compared to gait. D. Shape of high beta bursts during rest and gait showing higher peak amplitudes and narrow in regard to burst width during rest as compared to gait. Shaded error bars indicate SEM.

signed rank test: $p = 0.02$).

4.4. High beta band burst life-times are decreased during gait

To characterize gait-related changes in high beta band burst behavior, we compared life- and waiting-times across frequencies between gait and rest (Fig. 2C). The LWR is significantly reduced in the high beta band, while during rest, life-times of high beta bursts are longer, and waiting-times are reduced as compared to gait. An ANOVA with the factor task (rest/gait) showed a significant main effect of task ($F(1, 36) = 10.88$, $p = 0.002$) on LWR in the high beta band (20–30 Hz) across all 18 nuclei. A follow up Wilcoxon signed rank test confirmed significant differences ($p = 0.01$).

4.5. High beta band burst overall amplitude is decreased during gait

To investigate high beta band burst shape, we compared the average burst amplitude in the epoch around the burst peak across patients between gait and rest (Fig. 2D). We describe that overall amplitude as well as burst width are decreased during gait. We tested overall high beta burst amplitude across the whole epoch around the burst peaks and report a significant reduction during gait ($\chi^2(2) = 9$, $p = 0.002$, Wilcoxon signed rank test: $p = 0.005$).

4.6. Time-frequency power modulation during gait

Time-frequency group analysis of gait-cycle related oscillatory activity in the STN in relation to average resting baseline shows modulation at several frequencies (Fig. 3B). While low frequencies seem increased across the whole gait cycle, alpha (8–13 Hz) and low beta (13–20 Hz) oscillations show gait-cycle locked modulations relative to the resting baseline. However, these differences are not significant on a group level. Only high beta frequencies (20–30 Hz) show significant decreases ($p < 0.05$) across the whole gait-cycle (Fig. 3C) when compared to rest, confirming power spectral analysis results.

In relation to average gait baseline, gait-related time-frequency analysis displays a modulation pattern with alpha, beta and gamma frequency power being increased before and around the point of terminal contact of the foot contralateral to the respective STN. This lateralized modulation pattern is especially obvious when comparing contralateral and ipsilateral averaging results (Fig. 4).

This group average lateralized modulation pattern is a result of individual time-frequency modulations (see Supplementary material, Supplementary Figs. 3 and 4). Supplementary analysis shows that that signal modulations in both leads in the example subjects actually happen at the same time, regardless of laterality.

5. Discussion

This study shows that it is feasible to record neural activity from a sensing neurostimulator (Activa PC + S®, Medtronic, plc.) in parallel with kinematic measurements in freely moving PD patients and to detect gait cycle related changes in oscillatory power. We believe caution is necessary when interpreting the origin of the signal modulations during gait and argue that our results show physiological effects as well as technical artifacts.

5.1. High beta band oscillatory activity is attenuated during gait

To investigate the function of the STN during continuous walking, we describe changes of relative spectral power and percentage change of absolute power between gait and rest. Our power spectral analysis shows a significant attenuation of subthalamic high beta frequency power on the group level (Fig. 2A) and time-frequency analysis confirm

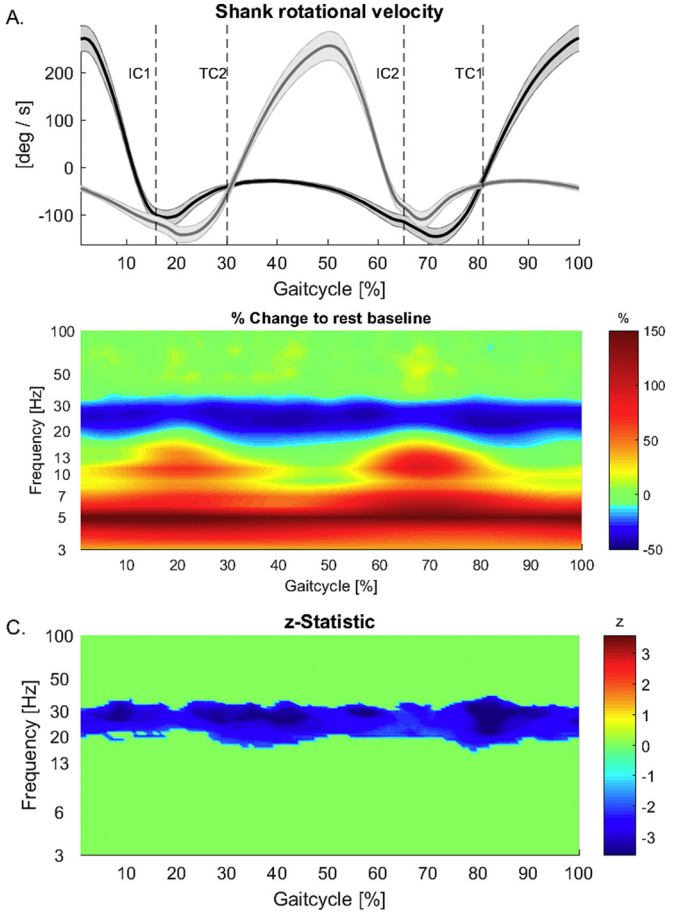

Fig. 3. A. Group shank rotation velocity. Gait cycle is epoched between the peak of the shank rotational velocity of one leg and the following peak of the same leg. Average contains epochs starting with left (e.g. Supplementary Fig. 3E) and right legs (e.g. Supplementary Fig. 3F). B, C. Time-frequency group analysis showing gait cycle locked modulation in relation to average resting using "contralateral averaging". While high beta frequency power is attenuated across the gait cycle, low frequencies show increases. Frequencies between 8 and 20 Hz do show increases in power in the double support periods of the gait-cycle. C. Group z-statistics for comparison between gait and rest showing significant decreases in power during gait in the high beta range (20–30 Hz) across the whole gait-cycle. Non significant z-values are zeroed out.

attenuation throughout the gait cycle (Fig. 3B, C). Evidence for beta power attenuation and gamma band increases in the cortex and basal ganglia during single movements come from various studies (Kühn et al., 2004; Litvak et al., 2012; Tan et al., 2016). Tan et al. described that oscillatory activity in the STN, particularly the gamma (55–90 Hz) and beta (13–30 Hz) band of the contralateral STN were most useful for decoding ipsilateral movement force during single movements. Earlier studies recording STN LFP during continuous movement suggest a reduction in beta frequency power during walking, particularly in akinetic-rigid, but not tremor dominant and freezing patients (Quinn et al., 2015; Singh et al., 2013; Storzer et al., 2017).

A few factors might influence inconsistency of findings in the literature. Tan et al. report that decoding was only successful in part of the recordings in which such a pattern was visible, but not in a second cluster, in which no significant movement-related modulation was observed in either the beta or gamma band. The mean frequency spectrum of the second group showed increased activity at low frequencies, extending to 25 Hz, particularly during the force onset phase. They argue that movement related artifacts are a possible cause for their observation of low frequency power increases at the time of movement onset, which also contaminated the beta band (Tan et al., 2016). It is

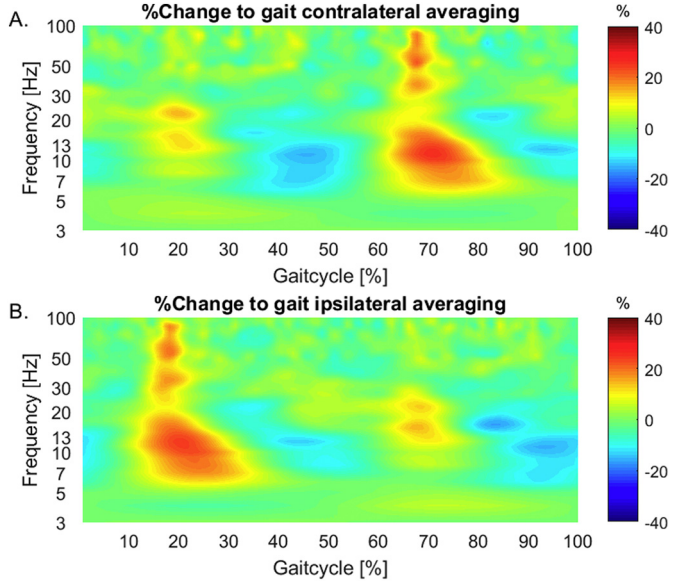

Fig. 4. A, B. Time-frequency group analysis showing gait cycle locked amplitude envelope modulation in relation to average gait baseline in alpha, beta and gamma frequencies using contralateral and ipsilateral averaging methods. For the average difference in A. signals from the left STN are used in epochs locked to right leg shank rotation peaks and right STN LFP in epochs beginning with the left foot (contralateral averaging). In B., the same analysis is presented, but using right STN LFPs for epochs which begin with right leg movement and vice versa (ipsilateral averaging).

conceivable that movement related artifacts (Fig. 4, Supplementary Figs. 3 and 4) during gait possibly also influence higher frequencies including beta and gamma and induce increases that obliterate physiological effects, therefore making it hard to detect such decreases. Another reason for the lack of consistent reports might be that these studies are conducted in PD patients, which are known to show elevated beta levels (Hammond et al., 2007). It has been shown, that excessive synchronization induced by low-frequency stimulation of subthalamic neurons at 20 Hz slows down movement in Parkinson's disease (Chen et al., 2007; Eusebio et al., 2008). Also, the development of bradykinesia during locomotion might be associated with a failure of beta attenuation. Confirming earlier reports, Steiner et al. showed that activity in the beta band was reduced during repetitive finger tapping, but reoccurred with the re-emergence of bradykinesia during prolonged tapping (Kühn et al., 2006b; Steiner et al., 2017).

5.2. High beta band bilateral connectivity is reduced during gait

With the investigation of differences in bilateral amplitude-amplitude correlations, we wanted to assess gait related changes in bilateral subthalamic oscillatory connectivity. Here, we report a reduction in bilateral amplitude-amplitude correlations in the high beta band during gait (Fig. 2B), confirming reports about movement-induced reduction in bilateral connectivity. Beta coherence between ipsilateral STN, globus pallidus internus and cortical regions has been reported to be attenuated by movement without dopaminergic medication. With medication however, beta levels are generally attenuated and power within the STN and coherence between the STN, globus pallidus internus and EEG was dominated by gamma band activity (70–85 Hz), increasing with movement (Cassidy et al., 2002; Lalo et al., 2008; Little et al., 2013b). While most studies focus on within hemisphere connectivity, other reports show that even unilateral movement results in bilateral changes in the STN, probably reflecting cortical input (Alegre et al., 2005). Niketeghad et al., report motor-modulated inter-hemispheric connectivity between bilateral STN LFP signals (Niketeghad et al., 2017). Hohlefeld and colleagues demonstrated coherence (iCOH)

between bilateral STN in the beta range (10–30 Hz). While iCOH in the 10–20 Hz frequency range positively correlated with the worsening of motor symptoms in the OFF medication condition, iCOH in the high beta range (21–30 Hz) was increased after levodopa administration (Hohlefeld et al., 2014). Hohlefeld et al. do not report on changes in oscillatory power. While this findings suggest a dissociation of low and high beta oscillations and relates only low beta oscillations to motor symptoms, our finding suggest that high beta oscillations are related to gait. The finding from Hohlefeld et al. stands in contrast with Little et al. (2013b), who also investigated the effects of levodopa medication on oscillatory power and interhemispheric connectivity in PD patients. Conversely, they report decreases in spectral power as well as decreases in standard coherence in the 13–20 Hz frequency band, but no significant changes in the high beta band. An ensuing question here is, if low and high beta band are indeed dissociable and have different functional relevance or other factors like interindividual variance (Haegens et al., 2014), small sample sizes or electrode location (Hohlefeld et al., 2014), contribute to the inconsistency and heterogeneity across reports.

5.3. High beta band burst life-times and burst amplitude are decreased during gait

Recently, it has been proposed to use pathological long beta bursts as a feedback signal for adaptive DBS (Meidahl et al., 2017; Tinkhauser et al., 2017a). The same group described that overall beta burst amplitude and duration in the STN are reduced by dopaminergic medication, while beta bursts with a long duration are decreased and short duration low amplitude bursts are increased (Tinkhauser et al., 2017b). We report that oscillatory characteristics are similarly affected during gait. We showed that the high beta burst amplitude and width is reduced during gait (Fig. 2D). Life-times of high beta bursts are reduced while waiting-times are increased, as indicated by significantly reduced LWR during gait (Fig. 2C). Together these findings indicate a reduction in burst strength and duration, mirroring differences found in recordings on and off dopaminergic medication.

5.4. Frequency modulation during gait

Here, we discuss the gait-cycle specific and seemingly lateralized modulation pattern (Fig. 4) of alpha, low beta and gamma frequencies that is time-locked to the gait-cycle. Power in alpha, beta and gamma frequencies is increased before and around the point of terminal contact of the foot contralateral to the respective STN.

Invasive electrophysiological studies reporting frequency amplitude modulations during movement and especially during gait are rare and conflicting. Androulidakis and colleagues showed that subthalamic oscillatory activity in the beta band was modulated in amplitude by finger tapping and this modulation probably failed as bradykinesia increased (Androulidakis et al., 2008). Florin et al. report increased activity in the low beta (12–18 Hz) and gamma (30–48 Hz) frequency ranges within the STN during fist flexion and extension and hypothesize that increases in gamma power enable repetitive fist movement despite increased beta levels (Florin et al., 2013). Storzer and colleagues report gait-cycle related STN power modulations in the 24–40 Hz range, which was correlated with EMG activity (Storzer et al., 2016). The same group also compared STN activity during bicycling and walking in PD patients with and without freezing of gait, affirming earlier reports. Patients without freezing of gait, in both bicycling and walking conditions, showed a suppression of subthalamic beta power (13–35 Hz). Freezers showed a similar pattern in general and an additional, movement-induced, narrowband power increase around 18 Hz time-locked to the onset of gait, reflecting earlier reports (Singh et al., 2013; Storzer et al., 2017). They argue that these results indicate that bicycling facilitates overall suppression of beta power and that specifically in patients susceptible to freezing, walking leads to exaggerated synchronization in the low beta band.

Our reported average group-level frequency dynamics seem to show a paradigmatic modulation pattern, partly overlapping with earlier studies on movement related frequency alterations. We want to argue that we are skeptical about the origin of the frequency power increases in our data and think that these considerations are relevant for similar research approaches. Previous invasive studies claim that movement related artifacts are restricted to low frequencies below 10 Hz (McCrimmon et al., 2017; Singh et al., 2011; Storzer et al., 2017). However, it has been previously shown that the influences of movement artifacts in electrophysiological signals on the frequency spectrum are not restricted to low frequency oscillations, but could indeed span several frequency ranges and are possibly time-locked to the gait cycle, using scalp EEG recordings (Castermans et al., 2013, 2012; Kline et al., 2015).

The lateralized modulation pattern visible in the group average (Fig. 4) is arguably driven by differences in artifact contamination across left and right STNs in individual subjects, as evidenced by stronger modulations in both the right STN in both example subjects (see Supplementary results and discussion). We think that movement artifact related noise influences electrophysiological recordings across setups – internal or external – that involve cables that can move or can be affected by tribo-electric effects and are extremely difficult to avoid completely. Together with putative physiological signal modulations (e.g. beta-power suppression), movement artifacts can induce frequency specific biases and lead to false positive results on a group level, especially with small group sizes. Various approaches, ranging from template subtraction to independent component analysis have been used to clean recordings from movement-related artifacts, but neither could conclusively show to disentangle physiological signals from technical noise (Castermans et al., 2013; Gwin et al., 2011, 2010; Snyder et al., 2015).

5.5. Beta oscillations as input for adaptive DBS

Our results do question if a threshold based on beta band oscillations alone is appropriate to use as a feedback mechanism in closed-loop DBS (Little et al., 2013a; Meidahl et al., 2017). Beta band oscillations are not only related to symptom severity, but also to medication (Kühn et al., 2008a, 2008b; Williams et al., 2005), cognition and movement (Foffani et al., 2005; Hell et al., 2018; Herz et al., 2016). Also, PD patients for example often show multiple symptoms, a single one-dimensional biomarker might therefore be only partly useful. Beta power in the STN correlates with rigidity and bradykinesia, but not with tremor (Lenka et al., 2016; Little and Brown, 2012), which is linked to low frequency activity at tremor frequency. Moreover, movement related noise can induce tonic changes in beta levels, furthermore complicating the use of oscillatory signals for adaptive deep brain stimulation. In addition to neuronal signals, kinematic measurements that might allow for the description of movement kinematics (for an analysis of movement parameters with and without DBS, see Supplementary material) and symptom severity could be a promising alternative or additional feedback signal for use in adaptive DBS. Inertial sensor measurements have already been successfully used for adaptive stimulation in essential tremor. While recording tremor amplitude and phase with inertial sensor units, Cagnan and colleagues stimulated patients with essential tremor and thalamic electrodes at specific phases of the tremor movement, successfully reducing tremor amplitude in a subset of patients (Cagnan et al., 2013).

By integrating features from electrophysiological recordings and kinematic measurements and other sensors like electromyography, the clinical state of the patient, the severity of disease symptoms and related neural activity might be ultimately learned and related to each other, using machine learning algorithms (Schirrmeister et al., 2017) and causal modelling approaches (Rubenstein et al., 2017). Stimulation parameters could be varied within clinical limits and those parameters

that are associated with optimal clinical state and neural parameters could then be learned via reinforcement learning.

5.6. Study limitations

This study was conducted in patients with Parkinson's disease which are known to show aberrant subthalamic oscillatory activity (Hammond et al., 2007) and problems during walking. Although patients were investigated after overnight withdrawal of medication, they were able to walk continuously without major impairments. We could show that our leads were placed in the posterior dorsal region and putative motor part of the STN (Accolla et al., 2016). It is still debated whether the subthalamic nucleus has distinct subregions, where exactly the motor subregion resides and what oscillatory mechanisms possibly reflect different subregions, networks and processes (Coenen et al., 2009; Greenhouse et al., 2011; Groppa et al., 2014; Horn et al., 2017; Jahanshahi et al., 2015; Lambert et al., 2012; Lanciego et al., 2012; Mallet et al., 2007; Plantinga et al., 2016).

6. Conclusion

The present study provides insight into subthalamic oscillatory dynamics during walking without and with stimulation and discusses the origin of the described signal modulations. We report persistent gait related attenuation of high beta frequency oscillations throughout the gait cycle, which is absent during stimulation (see Supplementary material). High beta band power and bilateral high beta connectivity are reduced during gait and oscillatory characteristics such as high beta burst amplitude and LWR follow the same pattern. Our analysis of gait cycle related oscillatory dynamics suggest that power in alpha, beta and gamma frequencies is increased before and around the point of terminal contact of the foot contralateral to the respective STN. Although our results overlap in part with previous reports, we argue that gait cycle locked signal increases we report here are driven by movement-related artifacts.

Conflict of interest

The authors declare no competing financial interests. The Activa PC + S devices used in this study were provided by Medtronic Europe.

Acknowledgements

We thank the patients for participating in this study. We also thank Ayse Bovet, Julia Cramer and Scott Stanslaski for their help in carefully proofreading the manuscript. F.H. was supported by the Lüneburg heritage.

Appendix A. Supplementary data

Supplementary data to this article can be found online at https://doi.org/10.1016/j.nicl.2018.05.001.

References

Accolla, E.A., Dukart, J., Helms, G., Weiskopf, N., Kherif, F., Lutti, A., Chowdhury, R., Hetzer, S., Haynes, J.-D., Kühn, A.A., Draganski, B., 2014. Brain tissue properties differentiate between motor and limbic basal ganglia circuits. Hum. Brain Mapp. 35, 5083–5092. http://dx.doi.org/10.1002/hbm.22533.

Accolla, E.A., Herrojo Ruiz, M., Horn, A., Schneider, G.-H., Schmitz-Hübsch, T., Draganski, B., Kühn, A.A., 2016. Brain networks modulated by subthalamic nucleus deep brain stimulation. Brain 139, 2503–2515. http://dx.doi.org/10.1093/brain/aww182.

Alegre, M., Alonso-Frech, F., Rodríguez-Oroz, M.C., Guridi, J., Zamarbide, I., Valencia, M., Manrique, M., Obeso, J.A., Artieda, J., 2005. Movement-related changes in oscillatory activity in the human subthalamic nucleus: ipsilateral vs. contralateral movements. Eur. J. Neurosci. 22, 2315–2324. http://dx.doi.org/10.1111/j.1460-9568.2005.04409.x.

Androulidakis, A.G., Brücke, C., Kempf, F., Kupsch, A., Aziz, T., Ashkan, K., Kühn, A.A., Brown, P., 2008. Amplitude modulation of oscillatory activity in the subthalamic nucleus during movement. Eur. J. Neurosci. 27, 1277–1284. http://dx.doi.org/10.1111/j.1460-9568.2008.06085.x.

Arnulfo, G., Hirvonen, J., Nobili, L., Palva, S., Palva, J.M., 2015. Phase and amplitude correlations in resting-state activity in human stereotactical EEG recordings. NeuroImage 112, 114–127. http://dx.doi.org/10.1016/j.neuroimage.2015.02.031.

Avants, B.B., Epstein, C.L., Grossman, M., Gee, J.C., 2008. Symmetric diffeomorphic image registration with cross-correlation: evaluating automated labeling of elderly and neurodegenerative brain. Med. Image Anal. 12, 26–41. http://dx.doi.org/10.1016/j.media.2007.06.004.

Benjamini, Y., Yekutieli, D., 2005. False discovery rate–adjusted multiple confidence intervals for selected parameters. J. Am. Stat. Assoc. 100, 71–81. http://dx.doi.org/10.1198/016214504000001907.

Bötzel, K., Marti, F.M., Rodríguez, M.Á.C., Plate, A., Vicente, A.O., 2016. Gait recording with inertial sensors - how to determine initial and terminal contact. J. Biomech. 49, 332–337. http://dx.doi.org/10.1016/j.jbiomech.2015.12.035.

Bötzel, K., Olivares, A., Paulo Cunha, J., Manuel Górriz Sáez, J., Weiss, R., Plate, A., 2018. Quantification of gait parameters with inertial sensors and inverse kinematics. J. Biomech. http://dx.doi.org/10.1016/j.jbiomech.2018.03.012.

Cagnan, H., Brittain, J.-S., Little, S., Foltynie, T., Limousin, P., Zrinzo, L., Hariz, M., Joint, C., Fitzgerald, J., Green, A.L., Aziz, T., Brown, P., 2013. Phase dependent modulation of tremor amplitude in essential tremor through thalamic stimulation. Brain 136, 3062–3075. http://dx.doi.org/10.1093/brain/awt239.

Cassidy, M., Mazzone, P., Oliviero, A., Insola, A., Tonali, P., Di Lazzaro, V., Brown, P., 2002. Movement-related changes in synchronization in the human basal ganglia. Brain 125, 1235–1246. http://dx.doi.org/10.1093/brain/awf135.

Castermans, T., Duvinage, M., Cheron, G., Dutoit, T., 2012. EEG AND HUMAN LOCOMOTION descending commands and sensory feedback should be disentangled from artifacts thanks to new experimental protocols position paper. In: Proceedings of the International Conference on Bio-inspired Systems and Signal Processing, pp. 309–314. http://dx.doi.org/10.5220/0003871403090314.

Castermans, T., Duvinage, M., Cheron, G., Dutoit, T., 2013. Towards effective non-invasive brain-computer interfaces dedicated to gait rehabilitation systems. Brain Sci. 4, 1–48. http://dx.doi.org/10.3390/brainsci4010001.

Chen, C.C., Litvak, V., Gilbertson, T., Kühn, A., Lu, C.S., Lee, S.T., Tsai, C.H., Tisch, S., Limousin, P., Hariz, M., Brown, P., 2007. Excessive synchronization of basal ganglia neurons at 20 Hz slows movement in Parkinson's disease. Exp. Neurol. 205, 214–221. http://dx.doi.org/10.1016/j.expneurol.2007.01.027.

Chung, K.K.K., Zhang, Y., Lim, K.L., Tanaka, Y., Huang, H., Gao, J., Ross, C.A., Dawson, V.L., Dawson, T.M., 2001. Parkin ubiquitinates the α-synuclein-interacting protein, synphilin-1: implications for Lewy-body formation in Parkinson disease. Nat. Med. 7, 1144–1150. http://dx.doi.org/10.1038/nm1001-1144.

Coenen, V.A., Honey, C.R., Hurwitz, T., Rahman, A.A., McMaster, J., Bürgel, U., Mädler, B., 2009. Medial forebrain bundle stimulation as a pathophysiological mechanism for hypomania in subthalamic nucleus deep brain stimulation for Parkinson's disease. Neurosurgery 64, 1106–1114. http://dx.doi.org/10.1227/01.NEU.0000345631.54446.06.

Costa, R.M., Lin, S.C., Sotnikova, T.D., Cyr, M., Gainetdinov, R.R., Caron, M.G., Nicolelis, M.A.L., 2006. Rapid alterations in corticostriatal ensemble coordination during acute dopamine-dependent motor dysfunction. Neuron 52, 359–369. http://dx.doi.org/10.1016/j.neuron.2006.07.030.

Espenhahn, S., de Berker, A.O., van Wijk, B.C.M., Rossiter, H.E., Ward, N.S., 2017. Movement-related beta oscillations show high intra-individual reliability. NeuroImage 147, 175–185. http://dx.doi.org/10.1016/j.neuroimage.2016.12.025.

Eusebio, A., Brown, P., 2009. Synchronisation in the beta frequency-band - the bad boy of parkinsonism or an innocent bystander? Exp. Neurol. 217, 1–3. http://dx.doi.org/10.1016/j.expneurol.2009.02.003.

Eusebio, A., Chen, C.C., Lu, C.S., Lee, S.T., Tsai, C.H., Limousin, P., Hariz, M., Brown, P., 2008. Effects of low-frequency stimulation of the subthalamic nucleus on movement in Parkinson's disease. Exp. Neurol. 209, 125–130. http://dx.doi.org/10.1016/j.expneurol.2007.09.007.

Feingold, J., Gibson, D.J., DePasquale, B., Graybiel, A.M., 2015. Bursts of beta oscillation differentiate postperformance activity in the striatum and motor cortex of monkeys performing movement tasks. Proc. Natl. Acad. Sci. 112, 13687–13692. http://dx.doi.org/10.1073/pnas.1517629112.

Florin, E., Erasmi, R., Reck, C., Maarouf, M., Schnitzler, A., Fink, G.R., Timmermann, L., 2013. Does increased gamma activity in patients suffering from Parkinson's disease counteract the movement inhibiting beta activity? Neuroscience 237, 42–50. http://dx.doi.org/10.1016/j.neuroscience.2013.01.051.

Foffani, G., Priori, A., Egidi, M., Rampini, P., Tamma, F., Caputo, E., Moxon, K.A., Cerutti, S., Barbieri, S., 2003. 300-Hz subthalamic oscillations in Parkinson's disease. Brain 126, 2153–2163. http://dx.doi.org/10.1093/brain/awg229.

Foffani, G., Bianchi, A.M., Baselli, G., Priori, A., 2005. Movement-related frequency modulation of beta oscillatory activity in the human subthalamic nucleus. J. Physiol. 568, 699–711. http://dx.doi.org/10.1113/jphysiol.2005.089722.

Fogelson, N., Pogosyan, A., Kühn, A.A., Kupsch, A., Van Bruggen, G., Speelman, H., Tijssen, M., Quartarone, A., Insola, A., Mazzone, P., Di Lazzaro, V., Limousin, P., Brown, P., 2005. Reciprocal interactions between oscillatory activities of different frequencies in the subthalamic region of patients with Parkinson's disease. Eur. J. Neurosci. 22, 257–266. http://dx.doi.org/10.1111/j.1460-9568.2005.04179.x.

Fonov, V., Evans, A.C., Botteron, K., Almli, C.R., McKinstry, R.C., Collins, D.L., 2011. Unbiased average age-appropriate atlases for pediatric studies. NeuroImage 54, 313–327. http://dx.doi.org/10.1016/j.neuroimage.2010.07.033.

Frank, M.J., 2006. Hold your horses: a dynamic computational role for the subthalamic nucleus in decision making. Neural Netw. 19, 1120–1136. http://dx.doi.org/10.1016/j.neunet.2006.03.006.

Frank, M.J., Samanta, J., Moustafa, A.A., Sherman, S.J., 2007. Hold your horses: impulsivity, deep brain stimulation, and medication in Parkinsonism. Science 318 (80), 1309–1312. http://dx.doi.org/10.1126/science.1146157.

Greenhouse, I., Gould, S., Houser, M., Hicks, G., Gross, J., Aron, A.R., 2011. Stimulation at dorsal and ventral electrode contacts targeted at the subthalamic nucleus has different effects on motor and emotion functions in Parkinson's disease. Neuropsychologia 49, 528–534. http://dx.doi.org/10.1016/j.neuropsychologia.2010.12.030.

Groppa, S., Herzog, J., Falk, D., Riedel, C., Deuschl, G., Volkmann, J., 2014. Physiological and anatomical decomposition of subthalamic neurostimulation effects in essential tremor. Brain 137, 109–121. http://dx.doi.org/10.1093/brain/awt304.

Groppe, D.M., Urbach, T.P., Kutas, M., 2011. Mass univariate analysis of event-related brain potentials/fields I: a critical tutorial review. Psychophysiology 48, 1711–1725. http://dx.doi.org/10.1111/j.1469-8986.2011.01273.x.

Gross, J., Pollok, B., Dirks, M., Timmermann, L., Butz, M., Schnitzler, A., 2005. Task-dependent oscillations during unimanual and bimanual movements in the human primary motor cortex and SMA studied with magnetoencephalography. NeuroImage 26, 91–98. http://dx.doi.org/10.1016/j.neuroimage.2005.01.025.

Gwin, J.T., Gramann, K., Makeig, S., Ferris, D.P., 2010. Removal of movement artifact from high-density EEG recorded during walking and running. J. Neurophysiol. 103, 3526–3534. http://dx.doi.org/10.1152/jn.00105.2010.

Gwin, J.T., Gramann, K., Makeig, S., Ferris, D.P., 2011. Electrocortical activity is coupled to gait cycle phase during treadmill walking. NeuroImage 54, 1289–1296. http://dx.doi.org/10.1016/j.neuroimage.2010.08.066.

Haegens, S., Cousijn, H., Wallis, G., Harrison, P.J., Nobre, A.C., 2014. Inter- and intra-individual variability in alpha peak frequency. NeuroImage 92, 46–55. http://dx.doi.org/10.1016/j.neuroimage.2014.01.049.

Hammond, C., Bergman, H., Brown, P., 2007. Pathological synchronization in Parkinson's disease: networks, models and treatments. Trends Neurosci. http://dx.doi.org/10.1016/j.tins.2007.05.004.

Hell, F., Taylor, P.C.J., Mehrkens, J.H., Bötzel, K., 2018. Subthalamic stimulation, oscillatory activity and connectivity reveal functional role of STN and network mechanisms during decision making under conflict. NeuroImage. http://dx.doi.org/10.1016/j.neuroimage.2018.01.001.

Herz, D.M., Zavala, B.A., Bogacz, R., Brown, P., 2016. Neural correlates of decision thresholds in the human subthalamic nucleus. Curr. Biol. 26, 916–920. http://dx.doi.org/10.1016/j.cub.2016.01.051.

Herz, D.M., Tan, H., Brittain, J.-S., Fischer, P., Cheeran, B., Green, A.L., FitzGerald, J., Aziz, T.Z., Ashkan, K., Little, S., Foltynie, T., Limousin, P., Zrinzo, L., Bogacz, R., Brown, P., 2017a. Distinct mechanisms mediate speed-accuracy adjustments in cortico-subthalamic networks. elife 6. http://dx.doi.org/10.7554/eLife.21481.

Herz, D.M., Tan, H., Brittain, J.-S., Fischer, P., Cheeran, B., Green, A.L., FitzGerald, J., Aziz, T.Z., Ashkan, K., Little, S., Foltynie, T., Limousin, P., Zrinzo, L., Bogacz, R., Brown, P., 2017b. Distinct mechanisms mediate speed-accuracy adjustments in cortico-subthalamic networks. elife 6. http://dx.doi.org/10.7554/eLife.21481.

Hohlefeld, F.U., Huchzermeyer, C., Huebl, J., Schneider, G.H., Brücke, C., Schönecker, T., Kühn, A.A., Curio, G., Nikulin, V.V., 2014. Interhemispheric functional interactions between the subthalamic nuclei of patients with Parkinson's disease. Eur. J. Neurosci. 40, 3273–3283. http://dx.doi.org/10.1111/ejn.12686.

Horn, A., Kühn, A.A., 2015. Lead-DBS: a toolbox for deep brain stimulation electrode localizations and visualizations. NeuroImage 107, 127–135. http://dx.doi.org/10.1016/j.neuroimage.2014.12.002.

Horn, A., Neumann, W.-J., Degen, K., Schneider, G.-H., Kühn, A.A., 2017. Toward an electrophysiological "sweet spot" for deep brain stimulation in the subthalamic nucleus. Hum. Brain Mapp. http://dx.doi.org/10.1002/hbm.23594.

Jahanshahi, M., Obeso, I., Rothwell, J.C., Obeso, J.A., 2015. A fronto–striato–subthalamic–pallidal network for goal-directed and habitual inhibition. Nat. Rev. Neurosci. 16, 719–732. http://dx.doi.org/10.1038/nrn4038.

Johnson, L.A., Nebeck, S.D., Muralidharan, A., Johnson, M.D., Baker, K.B., Vitek, J.L., 2016. Closed-loop deep brain stimulation effects on Parkinsonian motor symptoms in a non-human primate. Is beta enough? Brain Stimul. 9. http://dx.doi.org/10.1016/j.brs.2016.06.051.

Joundi, R.A., Brittain, J.S., Green, A.L., Aziz, T.Z., Brown, P., Jenkinson, N., 2013. Persistent suppression of subthalamic beta-band activity during rhythmic finger tapping in Parkinson's disease. Clin. Neurophysiol. 124, 565–573. http://dx.doi.org/10.1016/j.clinph.2012.07.029.

Kane, A., Hutchison, W.D., Hodaie, M., Lozano, A.M., Dostrovsky, J.O., 2009. Dopamine-dependent high-frequency oscillatory activity in thalamus and subthalamic nucleus of patients with Parkinson's disease. Neuroreport 20, 1549–1553. http://dx.doi.org/10.1097/WNR.0b013e32833282c8.

Kline, J.E., Huang, H.J., Snyder, K.L., Ferris, D.P., 2015. Isolating gait-related movement artifacts in electroencephalography during human walking. J. Neural Eng. 12, 046022. http://dx.doi.org/10.1088/1741-2560/12/4/046022.

Kühn, A.A., Williams, D., Kupsch, A., Limousin, P., Hariz, M., Schneider, G.H., Yarrow, K., Brown, P., 2004. Event-related beta desynchronization in human subthalamic nucleus correlates with motor performance. Brain 127, 735–746. http://dx.doi.org/10.1093/brain/awh106.

Kühn, A.A., Doyle, L., Pogosyan, A., Yarrow, K., Kupsch, A., Schneider, G., Hariz, M.I., Trottenberg, T., Brown, P., 2006a. Modulation of beta oscillations in the subthalamic area during motor imagery in Parkinson's disease. Brain 695–706. http://dx.doi.org/10.1093/brain/awh715.

Kühn, A.A., Kupsch, A., Schneider, G.H., Brown, P., 2006b. Reduction in subthalamic 8–35 Hz oscillatory activity correlates with clinical improvement in Parkinson's disease. Eur. J. Neurosci. 23, 1956–1960. http://dx.doi.org/10.1111/j.1460-9568.2006.04717.x.

Kühn, A.A., Brücke, C., Schneider, G.H., Trottenberg, T., Kivi, A., Kupsch, A., Capelle, H.H., Krauss, J.K., Brown, P., 2008a. Increased beta activity in dystonia patients after drug-induced dopamine deficiency. Exp. Neurol. 214, 140–143. http://dx.doi.org/10.1016/j.expneurol.2008.07.023.

Kühn, A.A., Kempf, F., Brücke, C., Gaynor Doyle, L., Martinez-Torres, I., Pogosyan, A., Trottenberg, T., Kupsch, A., Schneider, G.-H., Hariz, M.I., Vandenberghe, W., Nuttin, B., Brown, P., 2008b. High-frequency stimulation of the subthalamic nucleus suppresses oscillatory beta activity in patients with Parkinson's disease in parallel with improvement in motor performance. J. Neurosci. 28, 6165–6173. http://dx.doi.org/10.1523/JNEUROSCI.0282-08.2008.

Lalo, E., Thobois, S., Sharott, A., Polo, G., Mertens, P., Pogosyan, A., Brown, P., 2008. Patterns of bidirectional communication between cortex and basal ganglia during movement in patients with Parkinson disease. J. Neurosci. 28, 3008–3016. http://dx.doi.org/10.1523/JNEUROSCI.5295-07.2008.

Lambert, C., Zrinzo, L., Nagy, Z., Lutti, A., Hariz, M., Foltynie, T., Draganski, B., Ashburner, J., Frackowiak, R., 2012. Confirmation of functional zones within the human subthalamic nucleus: patterns of connectivity and sub-parcellation using diffusion weighted imaging. NeuroImage 60, 83–94. http://dx.doi.org/10.1016/j.neuroimage.2011.11.082.

Lanciego, J.L., Luquin, N., Obeso, J.A., 2012. Functional neuroanatomy of the basal ganglia. Cold Spring Harb. Perspect. Med. 2, a009621. http://dx.doi.org/10.1101/cshperspect.a009621.

Lenka, A., Hegde, S., Jhunjhunwala, K.R., Pal, P.K., 2016. Interactions of visual hallucinations, rapid eye movement sleep behavior disorder and cognitive impairment in Parkinson's disease: a review. Parkinsonism Relat. Disord. 22, 1–8. http://dx.doi.org/10.1016/j.parkreldis.2015.11.018.

Little, S., Brown, P., 2012. What brain signals are suitable for feedback control of deep brain stimulation in Parkinson's disease? Ann. N. Y. Acad. Sci. 1265, 9–24. http://dx.doi.org/10.1111/j.1749-6632.2012.06650.x.

Little, S., Pogosyan, A., Neal, S., Zavala, B., Zrinzo, L., Hariz, M., Foltynie, T., Limousin, P., Ashkan, K., Fitzgerald, J., Green, A.L., Aziz, T.Z., Brown, P., 2013a. Adaptive deep brain stimulation in advanced Parkinson disease. Ann. Neurol. 74http://dx.doi.org/10.1002/ana.23951. (n/a-n/a).

Little, S., Tan, H., Anzak, A., Pogosyan, A., Kühn, A., Brown, P., 2013b. Bilateral functional connectivity of the basal ganglia in patients with Parkinson's disease and its modulation by dopaminergic treatment. PLoS One 8, e82762. http://dx.doi.org/10.1371/journal.pone.0082762.

Litvak, V., Eusebio, A., Jha, A., Oostenveld, R., Barnes, G., Foltynie, T., Limousin, P., Zrinzo, L., Hariz, M.I., Friston, K., Brown, P., 2012. Movement-related changes in local and long-range synchronization in Parkinson's disease revealed by simultaneous magnetoencephalography and intracranial recordings. J. Neurosci. 32, 10541–10553. http://dx.doi.org/10.1523/JNEUROSCI.0767-12.2012.

Mallet, L., Schupbach, M., N'Diaye, K., Remy, P., Bardinet, E., Czernecki, V., Welter, M.-L., Pelissolo, A., Ruberg, M., Agid, Y., Yelnik, J., 2007. Stimulation of subterritories of the subthalamic nucleus reveals its role in the integration of the emotional and motor aspects of behavior. Proc. Natl. Acad. Sci. 104, 10661–10666. http://dx.doi.org/10.1073/pnas.0610849104.

Mallet, N., Pogosyan, A., Márton, L.F., Bolam, J.P., Brown, P., Magill, P.J., 2008. Parkinsonian beta oscillations in the external globus pallidus and their relationship with subthalamic nucleus activity. J. Neurosci. 28, 14245–14258. http://dx.doi.org/10.1523/JNEUROSCI.4199-08.2008.

Marceglia, S., Fiorio, M., Foffani, G., Mrakic-Sposta, S., Tiriticco, M., Locatelli, M., Caputo, E., Tinazzi, M., Priori, A., 2009. Modulation of beta oscillations in the subthalamic area during action observation in Parkinson's disease. Neuroscience 161, 1027–1036. http://dx.doi.org/10.1016/j.neuroscience.2009.04.018.

Maris, E., Oostenveld, R., 2007. Nonparametric statistical testing of EEG- and MEG-data. J. Neurosci. Methods 164, 177–190. http://dx.doi.org/10.1016/j.jneumeth.2007.03.024.

Maris, E., Schoffelen, J.M., Fries, P., 2007. Nonparametric statistical testing of coherence differences. J. Neurosci. Methods 163, 161–175. http://dx.doi.org/10.1016/j.jneumeth.2007.02.011.

McCrimmon, C.M., Wang, P.T., Heydari, P., Nguyen, A., Shaw, S.J., Gong, H., Chui, L.A., Liu, C.Y., Nenadic, Z., Do, A.H., 2017. Electrocorticographic encoding of human gait in the leg primary motor cortex. Cereb. Cortex 1–11. http://dx.doi.org/10.1093/cercor/bhx155.

Meidahl, A.C., Tinkhauser, G., Herz, D.M., Cagnan, H., Debarros, J., Brown, P., 2017. Adaptive deep brain stimulation for movement disorders: the long road to clinical therapy. Mov. Disord. 32, 810–819. http://dx.doi.org/10.1002/mds.27022.

Meijer, D., te Woerd, E., Praamstra, P., 2016. Timing of beta oscillatory synchronization and temporal prediction of upcoming stimuli. NeuroImage 138, 233–241. http://dx.doi.org/10.1016/j.neuroimage.2016.05.071.

Montez, T., Poil, S.-S., Jones, B.F., Manshanden, I., Verbunt, J.P.A., van Dijk, B.W., Brussaard, A.B., van Ooyen, A., Stam, C.J., Scheltens, P., Linkenkaer-Hansen, K., 2009. Altered temporal correlations in parietal alpha and prefrontal theta oscillations in early-stage Alzheimer disease. Proc. Natl. Acad. Sci. U. S. A. 106, 1614–1619. http://dx.doi.org/10.1073/pnas.0811699106.

Neumann, W.J., Staub, F., Horn, A., Schanda, J., Mueller, J., Schneider, G.H., Brown, P., Kühn, A.A., 2016. Deep brain recordings using an implanted pulse generator in Parkinson's disease. Neuromodulation 19, 20–23. http://dx.doi.org/10.1111/ner.12348.

Niketeghad, S., Hebb, A.O., Nedrud, J., Hanrahan, S.J., Mahoor, M.H., 2017. Motor task detection from human STN using interhemispheric connectivity. IEEE Trans. Neural Syst. Rehabil. Eng. http://dx.doi.org/10.1109/TNSRE.2017.2754879.

Oswal, A., Beudel, M., Zrinzo, L., Limousin, P., Hariz, M., Foltynie, T., Litvak, V., Brown, P., 2016. Deep brain stimulation modulates synchrony within spatially and spectrally distinct resting state networks in Parkinson's disease. Brain 139, 1482–1496. http://dx.doi.org/10.1093/brain/aww048.

Özkurt, T.E., Butz, M., Homburger, M., Elben, S., Vesper, J., Wojtecki, L., Schnitzler, A., 2011. High frequency oscillations in the subthalamic nucleus: a neurophysiological marker of the motor state in Parkinson's disease. Exp. Neurol. 229, 324–331. http://dx.doi.org/10.1016/j.expneurol.2011.02.015.

Pfurtscheller, G., Stancák, A., Neuper, C., 1996. Post-movement beta synchronization. A correlate of an idling motor area? Electroencephalogr. Clin. Neurophysiol. 98, 281–293. http://dx.doi.org/10.1016/0013-4694(95)00258-8.

Piña-Fuentes, D., Little, S., Oterdoom, M., Neal, S., Pogosyan, A., Tijssen, M.A.J., van Laar, T., Brown, P., van Dijk, J.M.C., Beudel, M., 2017. Adaptive DBS in a Parkinson's patient with chronically implanted DBS: a proof of principle. Mov. Disord. http://dx.doi.org/10.1002/mds.26959.

Plantinga, B.R., Temel, Y., Duchin, Y., Roebroeck, A., Kuijf, M., Jahanshahi, A., ter Haar Romenij, B., Vitek, J., Harel, N., 2016. Individualized parcellation of the subthalamic nucleus in patients with Parkinson's disease with 7T MRI. NeuroImage. http://dx.doi.org/10.1016/j.neuroimage.2016.09.023.

Priori, A., Foffani, G., Pesenti, A., Bianchi, A., Chiesa, V., Baselli, G., Caputo, E., Tamma, F., Rampini, P., Egidi, M., Locatelli, M., Barbieri, S., Scarlato, G., 2002. Movement-related modulation of neural activity in human basal ganglia and its L-DOPA dependency: recordings from deep brain stimulation electrodes in patients with Parkinson's disease. Neurol. Sci. 23, s101–s102. http://dx.doi.org/10.1007/s100720200089.

Quinn, E.J., Blumenfeld, Z., Velisar, A., Koop, M.M., Shreve, L.A., Trager, M.H., Hill, B.C., Kilbane, C., Henderson, J.M., Bronte-Stewart, H., 2015. Beta oscillations in freely moving Parkinson's subjects are attenuated during deep brain stimulation. Mov. Disord. 30, 1750–1758. http://dx.doi.org/10.1002/mds.26376.

Raz, A., Feingold, A., Zelanskaya, V., Vaadia, E., 1996. Neuronal synchronization of tonically active neurons in the striatum of normal and Parkinsonian primates. J. Neurophysiol. 76, 2083–2088.

Rubenstein, P.K., Weichwald, S., Bongers, S., Mooij, J.M., Janzing, D., Grosse-Wentrup, M., Schölkopf, B., 2017. Causal Consistency of Structural Equation Models.

Schirrmeister, R.T., Springenberg, J.T., Fiederer, L.D.J., Glasstetter, M., Eggensperger, K., Tangermann, M., Hutter, F., Burgard, W., Ball, T., 2017. Deep learning with convolutional neural networks for EEG decoding and visualization. Hum. Brain Mapp. http://dx.doi.org/10.1002/hbm.23730.

Sharott, A., Magill, P.J., Harnack, D., Kupsch, A., Meissner, W., Brown, P., 2005. Dopamine depletion increases the power and coherence of beta-oscillations in the cerebral cortex and subthalamic nucleus of the awake rat. Eur. J. Neurosci. 21, 1413–1422. http://dx.doi.org/10.1111/j.1460-9568.2005.03973.x.

Singh, A., Levin, J., Mehrkens, J.H., Bötzel, K., 2011. Alpha frequency modulation in the human basal ganglia is dependent on motor task. Eur. J. Neurosci. 33, 960–967. http://dx.doi.org/10.1111/j.1460-9568.2010.07577.x.

Singh, A., Plate, A., Kammermeier, S., Mehrkens, J.H., Ilmberger, J., Bötzel, K., 2013. Freezing of gait-related oscillatory activity in the human subthalamic nucleus. Basal Ganglia 3, 25–32. http://dx.doi.org/10.1016/j.baga.2012.10.002.

Snyder, K.L., Kline, J.E., Huang, H.J., Ferris, D.P., 2015. Independent component analysis of gait-related movement artifact recorded using EEG electrodes during treadmill walking. Front. Hum. Neurosci. 9. http://dx.doi.org/10.3389/fnhum.2015.00639.

Stein, E., Bar-Gad, I., 2013. Beta oscillations in the cortico-basal ganglia loop during parkinsonism. Exp. Neurol. http://dx.doi.org/10.1016/j.expneurol.2012.07.023.

Steiner, L.A., Neumann, W.J., Staub-Bartelt, F., Herz, D.M., Tan, H., Pogosyan, A., Kuhn, A.A., Brown, P., 2017. Subthalamic beta dynamics mirror Parkinsonian bradykinesia months after neurostimulator implantation. Mov. Disord. 32, 1183–1190. http://dx.doi.org/10.1002/mds.27068.

Storzer, L., Butz, M., Hirschmann, J., Abbasi, O., Gratkowski, M., Saupe, D., Schnitzler, A., Dalal, S.S., 2016. Bicycling and walking are associated with different cortical oscillatory dynamics. Front. Hum. Neurosci. 10. http://dx.doi.org/10.3389/fnhum.2016.00061.

Storzer, L., Butz, M., Hirschmann, J., Abbasi, O., Gratkowski, M., Saupe, D., Vesper, J., Dalal, S.S., Schnitzler, A., 2017. Bicycling suppresses abnormal beta synchrony in the Parkinsonian basal ganglia. Ann. Neurol. http://dx.doi.org/10.1002/ana.25047.

Tan, H., Jenkinson, N., Brown, P., 2014a. Dynamic neural correlates of motor error monitoring and adaptation during trial-to-trial learning. J. Neurosci. 34, 5678–5688. http://dx.doi.org/10.1523/JNEUROSCI.4739-13.2014.

Tan, H., Zavala, B., Pogosyan, A., Ashkan, K., Zrinzo, L., Foltynie, T., Limousin, P., Brown, P., 2014b. Human subthalamic nucleus in movement error detection and its evaluation during visuomotor adaptation. J. Neurosci. 34, 16744–16754. http://dx.doi.org/10.1523/JNEUROSCI.3414-14.2014.

Tan, H., Pogosyan, A., Ashkan, K., Green, A.L., Aziz, T., Foltynie, T., Limousin, P., Zrinzo, L., Hariz, M., Brown, P., 2016. Decoding gripping force based on local field potentials recorded from subthalamic nucleus in humans. elife 5. http://dx.doi.org/10.7554/eLife.19089.

Te Woerd, E.S., Oostenveld, R., Bloem, B.R., De Lange, F.P., Praamstra, P., 2015. Effects of rhythmic stimulus presentation on oscillatory brain activity: the physiology of cueing in Parkinson's disease. Neuroimage. Clin. 9, 300–309. http://dx.doi.org/10.1016/j.nicl.2015.08.018.

Tinkhauser, G., Pogosyan, A., Little, S., Beudel, M., Herz, D.M., Tan, H., Brown, P., 2017a. The modulatory effect of adaptive deep brain stimulation on beta bursts in Parkinson's disease. Brain 140, 1053–1067. http://dx.doi.org/10.1093/brain/awx010.

Tinkhauser, G., Pogosyan, A., Tan, H., Herz, D.M., Kühn, A.A., Brown, P., 2017b. Beta burst dynamics in Parkinson's disease OFF and ON dopaminergic medication. Brain. http://dx.doi.org/10.1093/brain/awx252.

Trager, M.H., Koop, M.M., Velisar, A., Blumenfeld, Z., Nikolau, J.S., Quinn, E.J., Martin, T., Bronte-Stewart, H., 2016. Subthalamic beta oscillations are attenuated after withdrawal of chronic high frequency neurostimulation in Parkinson's disease. Neurobiol. Dis. 96, 22–30. http://dx.doi.org/10.1016/j.nbd.2016.08.003.

Weiss, D., Klotz, R., Govindan, R.B., Scholten, M., Naros, G., Ramos-Murguialday, A., Bunjes, F., Meisner, C., Plewnia, C., Kruger, R., Gharabaghi, A., 2015. Subthalamic stimulation modulates cortical motor network activity and synchronization in Parkinson's disease. Brain 138, 679–693. http://dx.doi.org/10.1093/brain/awu380.

Williams, D., Kühn, A., Kupsch, A., Tijssen, M., Van Bruggen, G., Speelman, H., Hotton, G., Loukas, C., Brown, P., 2005. The relationship between oscillatory activity and motor reaction time in the Parkinsonian subthalamic nucleus. Eur. J. Neurosci. 21, 249–258. http://dx.doi.org/10.1111/j.1460-9568.2004.03817.x.

Zavala, B., Brittain, J.-S., Jenkinson, N., Ashkan, K., Foltynie, T., Limousin, P., Zrinzo, L., Green, A.L., Aziz, T., Zaghloul, K., Brown, P., 2013. Subthalamic nucleus local field potential activity during the Eriksen flanker task reveals a novel role for Theta phase during conflict monitoring. J. Neurosci. 33, 14758–14766. http://dx.doi.org/10.1523/JNEUROSCI.1036-13.2013.